ELSEVIER

Microelectronics Journal 39 (2008) 644–647

Microelectronics Journal

www.elsevier.com/locate/mejo

Reconfigurable 1×4 InP-based optical switch

D.A. May-Arrioja[a,*], P. LiKamWa[b]

[a]Photonics and Optical Physics Laboratory, Optics Department, INAOE, Apdo. Postal 51 y 216, Tonantzintla, Puebla 72000, Mexico
[b]CREOL & FPCE, The College of Optics and Photonics, University of Central Florida, Orlando, FL 32816, USA

Available online 20 August 2007

Abstract

An integrated 1×4 InP-based optical switch is reported. The device is quite simple and full device operation is achieved by injecting electrical currents to two electrodes. Since the operation of the switch relies on current spreading, using the carrier-induced refractive index change in InGaAsP multiple quantum wells, an area-selective zinc in-diffusion process is used to regulate the current spreading and optimize device performance. As a result, the fabricated 1×4 switch exhibits a -14 dB crosstalk between channels over a wavelength range of 30 nm, while maintaining low electrical power consumption and allowing the switch to be operated uncooled and under d.c. current conditions.

Keywords: Optical switch; Beam steering; Integrated optics; Multiple quantum wells; Carrier induced

1. Introduction

As a result of the continuous growth of telecom-based applications, such as internet and video on demand, the requirements for information transmission capacity have increased dramatically over the past two decades. The net result is the need for the deployment of high-capacity networks that can handle tremendous amount of information. A challenge for these networks is to offer high-speed routing capabilities that can handle such massive flows of information. Current technologies are reaching an upper limit as higher speeds are required. A more convenient way is to take advantage of the recent technological progress in advanced integrated photonic devices. Among the many photonic devices, photonic switches are becoming key components because they can perform a variety of applications, particularly in signal routing and time-division signal processing. In these applications, the optical transparency of photonic switch modules offers simplified and higher capacity system operation, by allowing networking function to be lowered to the optical layer. One of the major advantages of photonic switches is that they avoid the need for optical–electronic and electronic–optical (o–e–o) conversions. Such conversions not only limit the versatility and transparency of the system, but can also amount to signal deterioration and errors introductions. In fact, the elimination of such o–e–o conversions will result in a major decrease in the overall system cost, since the equipment associated with these conversions represents the main cost associated in today's networks.

Over the years different materials and configurations have been employed for the development of photonic switches. They can be separated by the physical switching mechanism, such as acousto-optic [1,2], thermo-optic [3,4], electro-optic [5,6], and even electro-mechanical in nature [7,8], depending on the application requirements. Several stand-alone switching devices have been demonstrated. However, another critical element in future optical networks is the integration of different photonic and electronic components on a single chip, the so-called photonic integrated circuits (PICs). PICs are becoming increasingly important, because this approach has the advantage that one obtains a small and compact unit in which all the components are connected by means of waveguides. This improves the robustness of the circuit, and reduces its sensitivity to the environment. Even more importantly, since packaging costs are a substantial, if not the main part of the component cost, it is more cost effective to integrate

*Corresponding author. Tel.: +52 222 247 2011x8115; fax: +52 222 247 2940.
E-mail address: dmay@inaoep.mx (D.A. May-Arrioja).

0026-2692/$ - see front matter © 2007 Elsevier Ltd. All rights reserved.
doi:10.1016/j.mejo.2007.07.047

multiple components monolithically within a single package. For PICs to become more attractive, the resulting chip should be able to process both optical and electronic signal. In this respect, III–V semiconductor based devices are the ideal candidates since they provide excellent properties for both photonic and electronic devices, and thus the possibility for highly integrated PICs [9].

In this work a versatile 1×4 optical switch based on InGaAsP multiple quantum wells (MQWs) is demonstrated. Switching was accomplished by steering the launched optical beam [10] and, redirecting it to any one of the four output waveguides. The switch exhibits a -14 dB crosstalk between channels over a wavelength range of 30 nm, while maintaining low electrical power consumption and allowing the switch to be operated uncooled and under d.c. current conditions. We believe that with further refinement of device design the device performance could be improved. More importantly, since the switch is patterned on an InP platform, it can be easily integrated with other photonic devices in order to implement a more sophisticated PICs.

2. 1×4 optical switch design

A schematic of the 1×4 optical switch is shown in Fig. 1. As illustrated, the 1×4 optical switching device can be divided into two primary sections; the beam steering section and the output waveguides. The beam steering section is composed of the input waveguide and a steering region. A laser beam entering the 4 μm wide input waveguide is launched into the exact center of the steering region, which consists of a slab waveguide with two parallel Ti/Au/Zn/Au top layer contact stripes, separated by 22 μm as measured from the inner edge of each stripe. The contact stripes are both 800 μm long and 10 μm wide. The output waveguides comprise the second section of the device. Each one is 4 μm wide and has a length of 500 μm. Initially, each output waveguide is separated by 2 μm, but as they spread out from the beam steering region, this value increases to 5 μm at the output facet. The wafer structure is grown on an n + InP substrate. It is composed of a 1 μm thick n-type InP buffer layer which are grown on 14 pairs of 100 Å thick, undoped, InGaAsP ($E_g = 0.816$ eV) quantum wells interspaced with 100 Å InGaAsP ($E_g = 1.08$ eV) barriers. The MQWs are topped by a 1.6 μm, n-type, InP cladding layer and a 100 nm InGaAs capping layer. The resulting slab waveguide is essentially symmetric, with all layers grown by metal organic chemical vapor deposition (MOCVD).

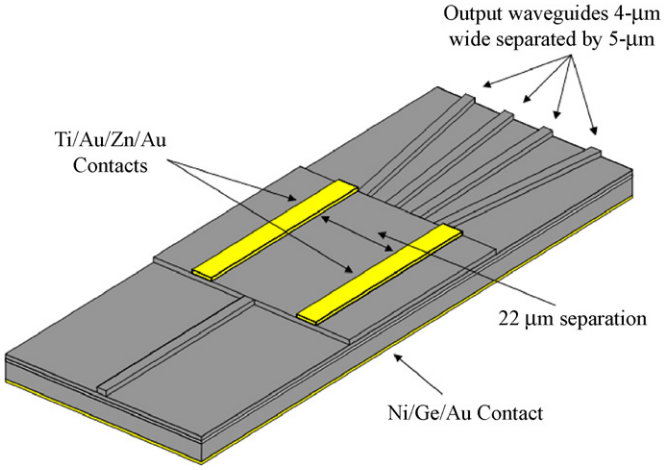

Fig. 1. Schematic of the 1×4 InP-based optical switch.

The device operates using the carrier-induced refractive index change in semiconductors [11]. When no current passes through the contact stripes, a 1.51 μm wavelength laser beam, launched into the steering region by the input waveguide, will expand into a slab mode. Lateral control and confinement of this beam is achieved by the application of an electrical current to each stripe. Zinc is previously diffused underneath the contact stripes in order to control the carrier spreading within the active region of the device. These diffused regions act to channel the electrons into the MQW layer and consequently enhance their efficiency in providing optical confinement and waveguiding. As current is applied, electrons are injected into the MQW layer where they then spread laterally through carrier diffusion. The areas within the active region that become saturated with electrons experience a corresponding decrease in refractive index. Carrier concentration is highest in the areas directly underneath the stripes, and decreases with lateral distance. This effectively results in the formation of a graded index channel waveguide between the two stripes in the steering region. Careful adjustment of the ratio between the currents applied to the two parallel contact stripes allows the waveguide to be shifted across the entire available range, thereby steering the signal beam. The input optical beam can then be directed to any of the output waveguides.

3. Device fabrication

Device fabrication began with the deposition of a silicon nitride diffusion mask for creating the zinc-diffused regions. Plasma-enhanced chemical vapor deposition (PECVD) was used to deposit a 200 nm thick silicon nitride film on the substrate surface. For each device, two $10\,\mu m \times 800\,\mu m$ diffusion windows were defined in the nitride film using conventional photolithography and CF_4 plasma-based reactive ion etching. The zinc in-diffusion process was carried out using a semisealed open-tube diffusion technique, similar to the one used in [10]. After the diffusion process was complete, the silicon nitride mask was removed and Ti/Au/Zn/Au p-type contacts were patterned on top of the zinc diffused areas by evaporation and lift-off. Photolithography was then used to pattern the input waveguide and output waveguide structures. Wet chemical etching with an H_3PO_4:H_2O_2:DI water (1:1:38) mixture was employed to selectively remove the InGaAs top layer. The remaining portions of the InGaAs layer were

then used as a mask for the selective wet etching of the InP using an $HCl:H_3PO_4:CH_3CHOHCOOH$ (2:5:1) mixture. A 10 nm InGaAsP etch stop layer, located 190 nm above the MQW layer, allowed precision control of the etch depth and yielded InP ridges of constant height, in addition to a smoothly etched surface. After etching was finished, the substrate was lapped to a thickness of 150 μm and polished to a mirror finish. Finally, the n-type contact consisting of Ni/Ge/Au was deposited via thermal evaporation and annealed in. The device sample was then cleaved and mounted on a copper header for testing.

4. Experimental results

The 1×4 optical switch was tested using an end-fire coupling technique using $40\times$ microscope objectives for coupling and collection of the optical power. The use of a $40\times$ microscope objective facilitates measuring the crosstalk between the output channels. A 50 μm diameter pinhole in front of the detector aperture guaranteed that only one channel could be measured at a time. The positioning of this detector could be adjusted along both the x- and y-axes, with the z-axis denoted as being parallel to the laser beam, so that the intensity in each of the four channels could be measured in turn. The approach employed in measuring the crosstalk required determining the current values needed to direct the laser beam to each of the four output waveguides. Then the current driver values were set to correspond to the first output waveguide and measurements of the light intensity in each of the four channels were measured through a lock-in amplifier. The current values were changed to send light to the next waveguide and the process was repeated until all channels had been likewise evaluated.

As can be observed in Fig. 2, by unbalancing the injected electrical currents, the laser beam can be easily directed to any one of the four output waveguides. The maximum current required was 38 mA, which is slightly higher if we compare it to the results obtained for a similar beam steering sub-unit [10]. This higher current is related to several factors. First, the separation between the electrodes in the 1×4 optical switch was 22 μm, as compared to 20 μm. This greater distance requires more current to form the transient waveguide. Furthermore, in [10] the beam steering section was optimized to achieve maximum steering with the lowest possible currents, not to achieve any predetermined confinement specification. In contrast, the current values selected for directing the laser beam to the individual output waveguides of the 1×4 switch were optimized to reduce the crosstalk. Therefore, higher currents were necessary in order to achieve a more confined mode. Irregardless of these issues, a current reduction better than six times was obtained as compared to a previous GaAs-based beam steering device that was fabricated without the zinc in-diffusion process [12]. A measured crosstalk of −14 dB was obtained for a wavelength range of 30 nm without the use of any cooling

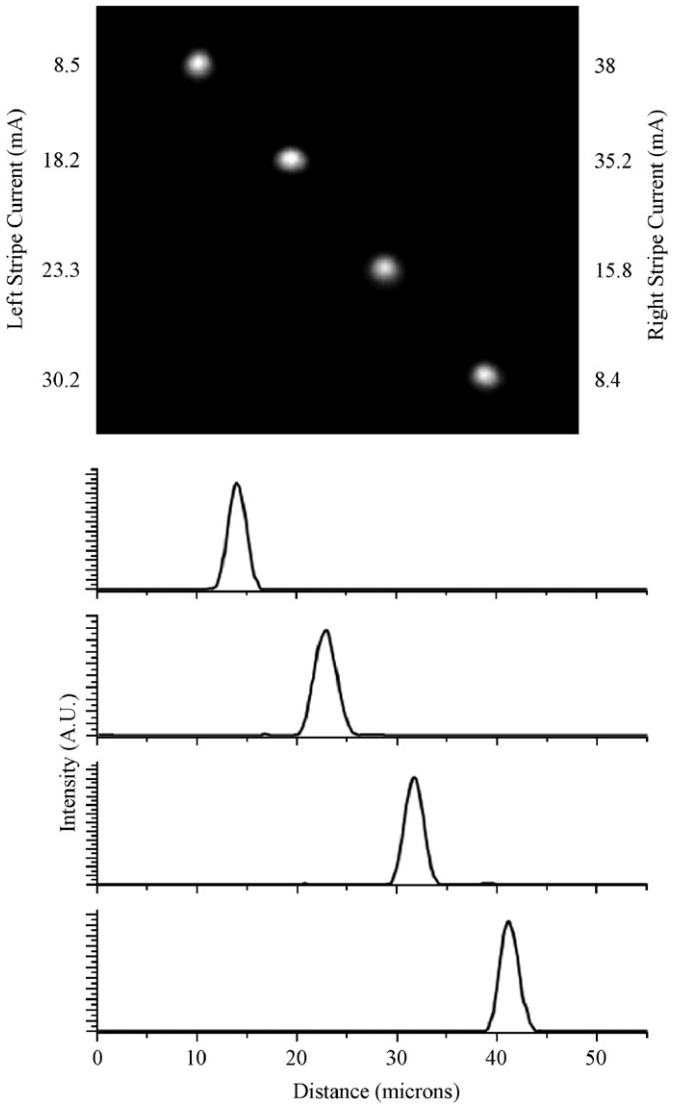

Fig. 2. Experimental results: (top) pictures of the near-field output facet at different applied currents, and (bottom) corresponding intensity profiles for the 1×4 optical switch.

mechanism and operating in d.c. current injection. Crosstalk can be improved if the bandwidth is reduced. Further improvement in device design should also provide a better crosstalk without reducing the bandwidth. Nevertheless, the results demonstrate a simple and reliable optical switch, which can be easily cascaded to develop $1 \times N$ or $N \times N$ switch fabrics. The key advantage of these devices relies on its potential for integration, which will be an added value for future optical networks.

5. Conclusions

A novel 1×4 optical switching device that operates with low driving current values using the principle of carrier-induced refractive index change in semiconductors has been demonstrated. The low power consumption resulted from the use of an area selective zinc in-diffusion process that acted to channel the current into the MQWs, thereby

enhancing the efficiency of the carrier-induced effects. A simple beam steering device was employed to direct the laser beam to the appropriate output channel. The lowest crosstalk obtained was −14 dB over a wavelength range of 30 nm. Improvements in our switch design should result in significant crosstalk reduction.

References

[1] G. Aubin, J. Sapriel, V.Y. Molchanov, R. Gabet, P. Grosso, S. Gosselin, Y. Jaouen, Multichannel acousto-optic cells for fast optical crossconnect, Electron. Lett. 40 (2004) 448–449.

[2] S. Gosselin, J. Sapriel, Versatile acousto-optic vector–matrix architecture for fast optical space switches, in: ECOC'98, Vol. 1, 1998, pp. 253–254

[3] T. Shibata, M. Okuno, T. Goh, T. Watanabe, M. Yasu, M. Itoh, M. Ishii, Y. Hibino, A. Sugita, A. Himeno, Silica-based waveguide-type 16×16 optical switch module incorporating driving circuits, IEEE Photon. Technol. Lett. 15 (2003) 1300–1302.

[4] C.H. Jang, R.T. Chen, Polymer-based 1×6 thermooptic switch incorporating an elliptic TIR waveguide mirror, J. Lightwave Technol. 21 (2003) 1053–1058.

[5] S. Akiyama, H. Itoh, T. Takeuchi, A. Kuramata, T. Yamamoto, Low-chirp 10 Gbit/s InP-based Mach–Zehnder modulator driven by 1.2 V single electrical signal, Electron. Lett. 41 (2005) 40–41.

[6] S. Abdalla, S. Ng, P. Barrios, D. Celo, A. Delage, S. El-Mougy, I. Golub, J.J. He, S. Janz, R. McKinnon, P. Poole, S. Raymond, T.J. Smy, B. Syrett, Carrier injection-based digital optical switch with reconfigurable output waveguide arms, IEEE Photon. Technol. Lett. 16 (2004) 1038–1040.

[7] P.B. Chu, S.S. Lee, S. Park, MEMS: the path to large optical crossconnects, IEEE Commun. Mag. 40 (2002) 80–87.

[8] P. De Dobbelaere, K. Falta, L. Fan, S. Gloeckner, S. Patra, Digital MEMS for optical switching, IEEE Commun. Mag. 40 (2002) 88–95.

[9] R. Kaiser, H. Heidrich, Optoelectronic/photonic integrated circuits on InP between technological feasibility and commercial success, IEICE Trans. Electron. E85-C (2002) 970–981.

[10] D.A. May-Arrioja, N. Bickel, P. LiKamWa, Optical beam steering using InGaAsP multiple quantum wells, IEEE Photon. Technol. Lett. 17 (2005) 333–335.

[11] B.R. Bennett, R.A. Soref, J.A. del Alamo, Carrier-induced change in refractive index of InP, GaAs, and InGaAsP, IEEE J. Quantum Electron. 26 (1990) 113–122.

[12] X. Dong, P. LiKamWa, J. Loehr, R. Kaspi, Current-induced guiding and beam steering in active semiconductor planar waveguide, IEEE Photon. Technol. Lett. 11 (1999) 809–811.